J Mater Sci (2011) 46:5595–5614
DOI 10.1007/s10853-011-5572-y

ANNIVERSARY REVIEW

# Review on polymer/graphite nanoplatelet nanocomposites

**Bin Li · Wei-Hong Zhong**

Received: 23 December 2010 / Accepted: 18 April 2011 / Published online: 4 May 2011


**Abstract** Graphite nanoplatelets (GNPs) are a type of graphitic nanofillers composed of stacked 2D graphene sheets, having outstanding electrical, thermal, and mechanical properties. Furthermore, owing to the abundance of naturally existing graphite as the source material for GNPs, it is considered an ideal reinforcing component to modify the properties of polymers. The 2D confinement of GNPs to the polymer matrix and the high surface area make the GNP a distinctive nanofiller, showing superiorities in modification of most properties, compared with other carbon nanofillers. This review will summarize the development of polymer/GNP nanocomposites in recent years, including the fabrication of GNPs and its nanocomposites, processing issues, viscoelastic properties, mechanical properties, electrical and dielectric properties, thermal conductivity and thermal stability. The discussion of reinforcing effect will be based on dispersion, particle geometry, concentrations, as well as the 2D structures and exfoliation of GNPs. The synergy of GNPs with other types of carbon nanofillers used as hybrid reinforcing systems shows great potential and could significantly broaden the application of GNPs. The relevant research will also be included in this review.

## Introduction

As one of the most important branches of current nanotechnology and composite science, the fabrication of polymer nanocomposites is critical to realizing the new generation materials with high performances and multifunctionalities. By incorporating nanofillers in a polymer matrix, we can combine the light weight, flexibility, and transparency of polymers with the excellent mechanical, physical, and other properties of nanomaterials [1–10]. Great research efforts on polymer nanocomposites in past decades have shown fruitful achievements in improving mechanical properties, thermal stability, electrical and thermal conductivities, dielectric performances, gas barrier property, and other attributes [11–16].

Graphite nanoplatelets (GNPs), also called graphite nanosheet (GN) and graphite nanoflake (GNF), or just simply exfoliated or expanded graphite (EG), is a type of 2D graphitic nanofiller consisting of stacked graphene layers. The stacked layers are bonded to each other by weak Van der Waals forces with a constant interlayer distance of ca. 0.34 nm [3]. The thickness of GNPs varies from several to dozens of nanometers, as compared to their diameter, usually in the microscale, which leads to the high specific surface area of GNPs (with a theoretical value of 2630–2965 $m^2/g$ [1]) and high aspect ratios. The thickness and diameter of GNPs could be tuned by a variety of techniques, such as intercalation, oxidization, heat treatment, microwave irradiation, and ultrasonic treatment, etc. [17–20]. Compared with other classic 2D nanofillers, such as nanoclays, GNPs have lower mass density, and are highly electrically and thermally conductive, due to the $sp^2$ hybridized carbons in the monolayer graphenes within the GNPs. The graphene also possesses superior mechanical properties with a reported modulus of 1100 GPa and strength of 125 GPa [21]. Therefore, GNPs are truly ideal for improving the properties of polymers and realizing multifunctionalities for practical applications. Furthermore, unlike other graphitic carbon nanofillers, such as carbon nanotubes and carbon nanofibers, the production of which usually requires expensive and intricate apparatus, as well

B. Li · W.-H. Zhong (✉)
School of Mechanical and Materials Engineering,
Washington State University, Pullman, WA 99164, USA
e-mail: Katie_Zhong@wsu.edu

as high energy consumption (chemical vapor decomposition, arc-discharging, laser ablation, etc. [22–24]), high-purity GNPs can also be derived from the plentiful resource of natural graphite by relatively convenient approaches [1, 8]. This makes the GNPs a type of cost-effective nanofiller to potentially replace high-priced carbon nanotubes in many key applications.

The development of polymer/GNP nanocomposites has been an ardent research subject in past years [25–29]. Especially, after the monolayer graphene with unique and extraordinary electronic structures and superior mechanical properties was successfully fabricated in 2004 [30], the relevant research has boomed. Tremendous amounts of work have been carried out on the preparation of monolayer graphene sheets, GNPs containing only very few sheets, or corresponding oxides [21, 31–36], to fully explore the potential of these 2D graphitic nanofillers in advanced polymer nanocomposites. However, because of the big challenges of manufacturing monolayer graphenes (or only very few layers) without compromising their properties, the practical applications of graphene-modified polymer nanocomposites still need more effort. The current status of polymer/graphene composites has recently been reviewed in [31]. Polymer/GNP nanocomposites are showing more practical applications today, due to both the extraordinary properties and the ease of fabrication of GNPs as mentioned above. This review will aim at providing a comprehensive understanding of recent research on polymer/GNP composites since 2004, including fabrication of GNPs, fabrication of polymer/GNP nanocomposites, various properties, among which, the latter two will be discussed in detail.

## Approaches to GNPs

Although GNPs can be synthesized through chemical vapor deposition [31] and arc discharging methods [19], among others (just as other graphitic carbon nanofillers, owing to the plentiful graphite in nature), two fabrication approaches are most preferred: mechanical milling and graphite-intercalation chemistry approaches. Mechanical milling [8] is a top-down process by breaking up bulk graphite, especially breaking the Van de Waals force. The resulting GNPs have the disadvantages of large particle size and a broad particle size distribution. These problems could be readily improved by the graphite-intercalation approach, which starts from the intercalation of graphite to obtain graphite intercalate compound (GIC). The basis of intercalation is to "place" some chemicals within the natural graphite layers. These chemicals are able to react and yield either a large volume of gas or enormous heat to force the separation of adjacent graphene layers. Acid intercalation (Fig. 1) is the most mature and commonly used technique for this purpose [37]. It is usually done by immersing natural graphite in concentrated/fumed sulfuric acid ($H_2SO_4$) solution containing various oxidizers such as concentrated nitric acid ($HNO_3$), $KMnO_4$, $H_2O_2$, $O_3$, etc. The acid intercalation can also be carried out by vapor

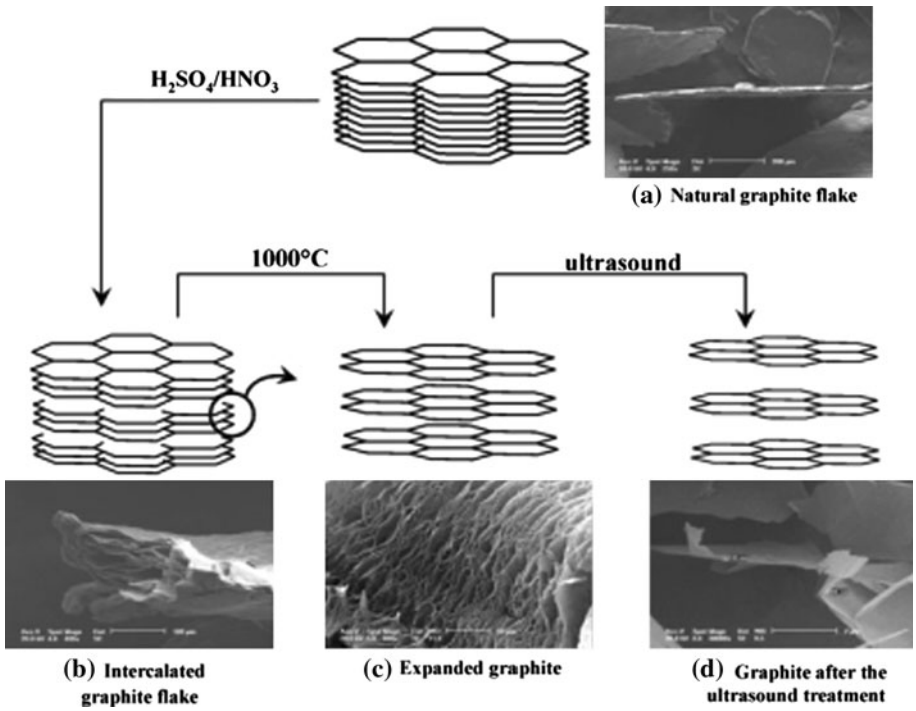


**Fig. 1** Scheme of the graphite structure modification after different treatments [3]

phase reaction and electrochemical methods. The intercalation is accomplished by following model equations [17]:

$$pC + [Ox] \rightarrow C_p^+ + [Ox]^-, \quad (1)$$

$$C_p^+ + A^- + mHA \rightarrow C_p^+A^- \cdot mHA. \quad (2)$$

where $p$ represents the numbers of carbon atoms needed to form macrocations ($C_p^+$) in carbon layers, and $m$ represents the number of acid molecules needed to form GIC. Followed by the rapid heating of GIC to above 1000 °C, the GIC will dramatically expand due to the generation of a great amount of gases including $SO_2$ and $H_2O$. Usually, this process only lasts for about 20–30 s. The product of expanded graphite typically has a worm-like morphology [20]. The heat expansion could be carried out in both air and nitrogen atmosphere. The latter condition will partially reduce the graphite oxide formed during acid intercalation. Besides heat expansion, microwave irradiation is also believed to provide sufficient energy to promote the expansion of GIC, with larger volume exfoliation ratio and less sulfur residue, compared with heat expansion [38, 39]. Lastly, to obtain GNPs, high intensity ultrasonication will be applied for a sufficiently long time to break down the expanded graphite (Fig. 1). The ultrasonication power and duration have significant impact on the size of GNPs.

The alkali metals and compounds are another good choice to be used as an intercalant to prepare the GIC [1, 40]. Typically, by heating the graphite powder and potassium (K), the intercalant compound, $KC_8$, appears as shown in Fig. 2. The expansion of GIC could be done using aqueous exfoliating agents, such as water and alcohol. Equation 3 gives the reaction happening between $KC_8$ and alcohol. Obviously, the yielded $H_2$ gas could break the weak Van der Waals force bonding within the graphite and lead to the exfoliation of graphite. Owing to the formation of potassium ethoxide, the exfoliated graphite is usually washed several times until the pH value is neutral. Other alkali metals involved for this purpose include Cesium (Cs) and sodium-potassium compound ($NaK_2$) [1]. The alkali metals can also be used in graphite already intercalated and exfoliated by acids for a double intercalation/exfoliation, to produce much thinner GNPs. After expansion, the resulting GNPs particles could have a length of 2–20,000 μm, compared with 0.4–60 μm for micro-graphite sheets [41].

$$KC_8 + CH_3CH_2OH \rightarrow 8C + KOCH_2CH_3 + {}^1/_2H_2 \quad (3)$$

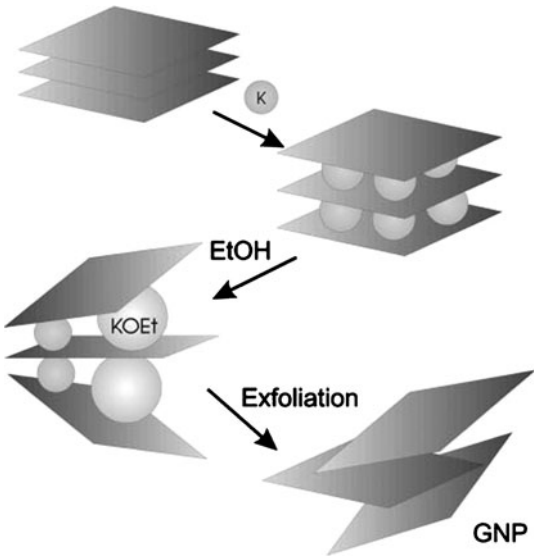


**Fig. 2** Schematic diagram showing the intercalation and exfoliation process to produce graphite nanoplatelets (GNP). Graphite is intercalated with potassium metal to form the first stage compound $KC_8$. Exfoliation in ethanol produces potassium ethoxide and hydrogen gas which aid in separating the graphitic sheets to form graphite nanoplatelets [1]

## Fabrication of polymer/GNP nanocomposites

Just like all other types of polymer nanocomposites, the main issue in the fabrication of polymer/GNP nanocomposites is still the dispersion and distribution of GNPs in the polymer matrix. Conventional techniques including in situ polymerization, solution mixing, and melt mixing are notably suitable for GNP-filled polymer nanocomposites. In particular, the porous nature of GNPs [42] allows the penetration of monomers and polymer chains into GNPs (Fig. 3), thus, the in situ polymerization and solution mixing with assistance of ultrasonication have shown great superiority in achieving highly homogeneous dispersion of GNPs, and full intercalation by polymer matrix (more interaction among GNPs and polymer matrix) [2, 38, 43–45]. They also appear ideal to process thermosetting polymer/GNP nanocomposites [7, 46–48]. Specifically, the fabrication of thermosetting polymers/GNPs starts from dispersing GNPs in liquid monomers of thermosetting polymer via solution mixing, followed by in situ polymerization to obtain crosslinked thermosetting polymer/GNPs composites. This often leads to polymer/GNP nanocomposites fabricated by these two approaches showing very low percolation thresholds of electrical conductivity and high electrical conductivity post percolation. The details are provided in Table 1 in "Electrical conductivity" of the electrical properties of polymer/GNP nanocomposites. A comprehensive improvement of mechanical and physical properties (electrical and thermal) of elastomer/GNP nanocomposites by latex compounding techniques was also observed, compared with direct melt mixing approach [39].

However, these two approaches also face some critical problems: (1) hazardous chemicals are necessarily involved, either monomers for polymerization or organic

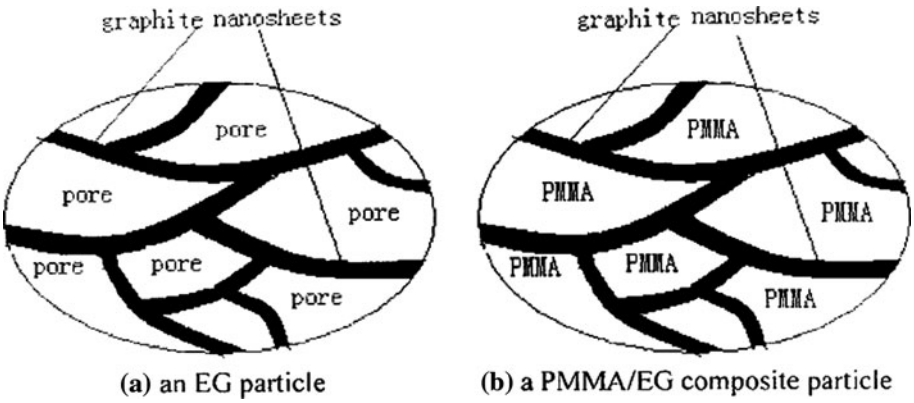


**Fig. 3** Formation process diagram of PMMA/GNP composite. **a** The section diagram of an GNP particle; **b** the section diagram of a PMMA/GNP composite particle [42]

**Table 1** Mechanical properties of pure epoxy and GNP/epoxy composites [68]

| Properties | Epoxy | GP/epoxy composites | | | |
|---|---|---|---|---|---|
| | | 0.5 wt%GP | 1 wt%GP | 2 wt%GP | 5 wt%GP |
| Flexural modulus (GPa) | 2.48 ± 0.19 | 2.51 ± 0.15 | 2.66 ± 0.23 | 2.70 ± 0.03 | 2.80 ± 0.07 |
| Increment (%) | | 1.2 | 7.3 | 8.9 | 13.0 |
| Flexural strength (MPa) | 92.90 ± 17.20 | 110.68 ± 14.19 | 114.33 ± 9.71 | 127.55 ± 11.34 | 134.93 ± 7.05 |
| Increment (%) | | 19.1 | 23.0 | 37.3 | 45.2 |
| Strain to failure (%) | 0.049 ± 0.007 | 0.053 ± 0.009 | 0.052 ± 0.010 | 0.062 ± 0.006 | 0.063 ± 0.007 |
| Increment (%) | | 8.2 | 6.1 | 6.5 | 28.6 |
| Toughness ($MPam^{1/2}$) | 1.26 ± 0.03 | 1.49 ± 0.02 | 1.52 ± 0.07 | 1.51 ± 0.04 | 1.61 ± 0.04 |
| Increment (%) | | 18.3 | 20.6 | 19.8 | 27.8 |

solvent as processing medium; (2) they are not ideal for industry production, owing to the low yield and high production cost. Thus, there is still a huge demand for fabrication techniques based on melt mixing. Much research has proved that the direct melt mixing is not sufficient for a satisfactory dispersion quality and properties of resultant polymer/GNP nanocomposites. A series of modified melting compounding techniques have been developed, which have shown remarkable improvement compared with direct mixing [49–53]

Two-step melt mixing techniques with various premix procedures (first step) before melt mixing (second step) have been developed to overcome the shortcomings of the direct melt mixing. The premix procedure can be accomplished in solution, melt, and solid. Drzal and co-workers [4] developed a novel coating approach, in which, the GNPs and polypropylene (PP) powder are premixed in the isopropyl alcohol with sonication to disperse GNPs by coating individual PP particles, prior to any melt compounding (injection molding, compression molding, etc.). The nanocomposites fabricated by this coating approach had much better flexural properties compared with those fabricated by direct melt mixing method. As for the electrical properties, the coating approach was even superior to the solution method, showing high electrical conductivity at same loading. A master batch filling technique also proved effective in improving the dispersion of GNPs and properties of nanocomposites. In this technique, a polymer master batch containing high content of GNPs (60 wt%) was first prepared, followed by diluting the master batch in the polymer matrix via melt mixing method. The high density polyethylene (HDPE)/GNP composites and Acrylonitrile-Styrene copolymer (AS)/GNP composites have been successfully fabricated by this method [54, 55]. A solid-state shear pulverization (SSSP) [56–59], originally used to improve the compatibility of polymer blends, also has been successful in polymer nanocomposites. The manually blended polymer pellets and nanofiller powders undergo compression and high shear/extensional conditions in a pulverizer at a temperature below melting temperature (semi-crystalline polymer) or glass transition temperature (amorphous polymer), resulting in a fine powder output without melting. The resultant fine powder of the mixture is further mixed and molded into desired polymer nanocomposites with improved dispersion quality and properties. PP/GNP nanocomposites fabricated by this SSSP method enormously surpass the same nanocomposites fabricated by direct mixing in tensile properties, impact toughness, and the ability to crystallize [56]. Furthermore, a harsh SSSP processing is more effective to exfoliate and

disperse GNP particles in PP matrix, compared with a mild one, achieving a GNP network structure at a low loading, better thermal stability as well as higher crystallization speed [59].

In the fabrication of polymer nanocomposites, the surface modification of nanofillers is also an important issue to strengthen the interaction between polymer matrix and nanofillers and resulting in better dispersion quality and high performances. By acid intercalant-assisted exfoliation, currently the most productive and commercially favorable approach is to produce high-quality GNPs, the oxidization of GNPs produced is unavoidable, leading to graphite oxide products with GNPs attached to many hydroxyl, epoxides, and carbonyl groups. These functional groups, on one hand, could form some strong interaction with polymer matrix containing polar groups; on the other hand, they provide reactive sites for further surface modification. So far, a great amount of various chemicals have been used for surface modification of GNPs, including octadecylamine (ODA) [2], maleated ethylene-propylene copolymer (EP-g-MA) [50], PP-g-MAH [51], unsaturated polyester resin [60], among others. However, the surface modification based on the graphite oxide is usually deleterious to the physical properties of GNPs, due to the transformation from $sp^2$ to $sp^3$ carbons during acid oxidization, the latter of which is far less conductive. The approach used for fabricating poly(arylene disulfide) (PAD)/graphite nanocomposite by Meng and co-workers [61] seems to be an ideal alternative to combine the good dispersive ability of GNP oxide and good physical properties of GNPs. In this approach, they produced PAD/GNP oxide nanocomposites first, and then the corresponding PAD/GNP nanocomposites could be obtained by heat treatment under dynamic vacuum at 473 K to reduce the oxide to graphene structures. The electrical conductivity showed a dramatic increase from $10^{-7}$ S/cm to 0.51 S/cm after the heat treatment reduction.

## Properties of polymer/GNP nanocomposites

### Melt viscosity/processibility

The melt viscosity of polymers and their composites is a critical property essentially impacting the processibility and production costs, as well as the microstructural characteristics and properties of polymer composites. Like all rigid fillers, the addition of GNPs in a polymer matrix will increase the melt viscosity, and correspondingly the difficulty of fabricating polymer/GNP nanocomposites. The increasing viscosity with GNP concentration is related to the formation of the GNP network in the polymer melt which strongly depends on the aspect ratio and the degree of exfoliation of GNP [5, 16, 44, 49–53]. Figure 4 schematically illustrates the structural evolution of GNPs during fabrication of TPV/PP-g-MA/GNP nanocomposites [51], which could represent most delamination processes of GNPs during processing. The high aspect ratio delaminated GNPs in polymer melt causes the formation of a GNP network at a very low loading level, compared with micro-graphite/polymer composites, leading to the much higher melt viscosity of polymer/GNP nanocomposites. The formation of GNP networks in polymer melt at low loading levels also affects the rheological properties which will be discussed in the next section of the viscoelastic behavior.

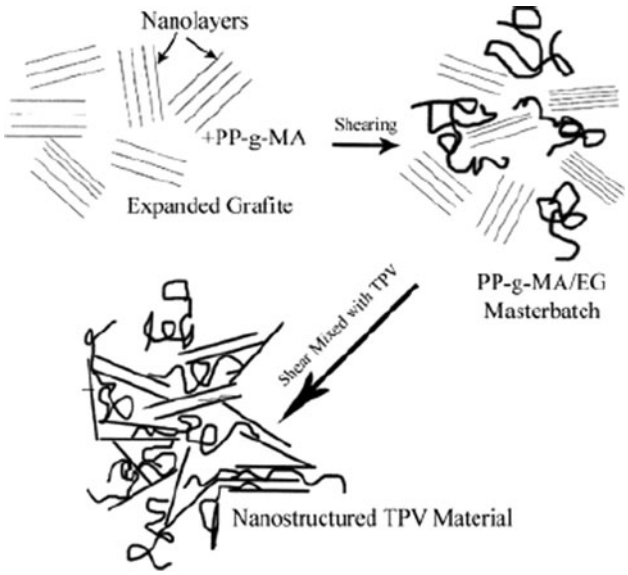


**Fig. 4** Model showing the morphology development during melt mixing of g-PP/GNP (EG nanoparticles) master batch (ME) and santoprene thermoplastic vulcanizate (TPV) [51]

Although all the carbon nanofillers show great mechanical and physical properties, due to their different micro-/nano-structures, their impact on the melt viscosity/processibility is distinctly different. Some research [16, 62] has already found out that, compared with carbon black, carbon nanofibers and carbon nanotubes, GNP-filled polymer nanocomposites have the lowest melt viscosity in a certain range of filler loadings, indicating better processibility. This associates with the ability of different nanostructures in various polymers to form network structures that could constrain the motions of polymer chains. A possible reason for the lower viscosity is that 2D graphitic structure might also act as a solid lubricant [50].

### Viscoelastic properties

Rheological behavior (complex viscosity, storage, and loss modulus) of polymer composites strongly depends on the formation and evolution of network structures of fillers in

polymer melt with strain, time, and temperature. Normally, the increasing loading of GNPs in polymer melts could gradually lead to a liquid–solid transformation, due to the mechanically stable network formed by GNPs interacting with polymer chains. Specifically, at low loading, the storage modulus of the composite melt is frequency dependent at low frequencies, the same as pure polymer melt. As the loading goes up, the network of GNPs will form step by step, and the frequency dependence of storage modulus at low frequency will finally diminish, indicating a typical solid-like behavior, as shown in Fig. 5 [53]. At the same time the complex viscosity starts to show shear thinning behavior [53]. The critical concentration for this transition is directly related with the aspect ratio of GNPs by equation [26, 53, 63]:

$$A_f = \frac{2r}{h} = \frac{3\phi_{\text{sphere}}}{2\phi_{\text{per}}} \tag{4}$$

where $A_f$ is the aspect ratio, $r$ and $h$ are the radius and thickness of GNP, respectively; $\phi_{\text{sphere}} = 0.29$ is the onset of the percolation of interpenetrating, randomly packed spheres; $\phi_{\text{per}}$ is the percolation threshold of GNPs (rheological percolation). The high degree of exfoliation usually leads to high aspect ratio and a greater number of GNPs in a polymer melt, both of which could accelerate the formation of GNP networks. Consequently, the high modulus and viscosity, as well as low percolation threshold of liquid–solid transition is not unexpected [59]. This is why much more micro-graphite fillers are needed in a polymer melt to reach the similar modulus and viscosity levels of GNP-filled polymer nanocomposites with low loading [31, 53]. Besides processing parameters, the degree of exfoliation of GNPs also strongly depends on GNP-polymer interactions, thus, different polymer/GNP nanocomposite systems have shown different rheological percolation threshold [31, 51, 53, 59].

Dynamic mechanical analysis (DMA) is used to evaluate the viscoelastic properties of polymer nanocomposites below and around the glass transition. Generally, for polymer nanocomposites, dispersion, interface bonding between polymer and nanofillers, and concentration are fundamental aspects impacting the dynamic mechanical properties, similar to all other types of nanofillers. At the same time, owing to the 2D nature and multiple layer structure of GNPs, additional structural factors also account for the variations of dynamic mechanical properties.

Both storage modulus and loss modulus increase with the loading of GNPs [7, 8, 10, 20, 64, 65]. The contribution of the addition of GNPs to the increase of storage modulus is due to two primary reasons. First, the interaction between polymer matrix and nanofillers could restrict the mobility of polymer chains around or absorbed on the surface of GNPs, leading to the formation of a stiffened interphase. In particular, the 2D GNPs have a relatively large surface area which could facilitate the absorption of polymers (Fig. 6). Secondly, at higher loading, owing to the formation of GNP networks inside the polymer matrix, the high storage modulus of GNPs is also be involved in the increased modulus of polymer/GNPs nanocomposites [20]. Both reasons are affected by dispersion, concentration, size, and degree of exfoliation of GNPs. Better dispersion, smaller particle size, and higher degree of exfoliation benefit the formation of stronger interfacial bonding (more stiffened interface area) as well as effective GNP networks, and correspondingly higher modulus. Especially noteworthy, improving the degree of exfoliation

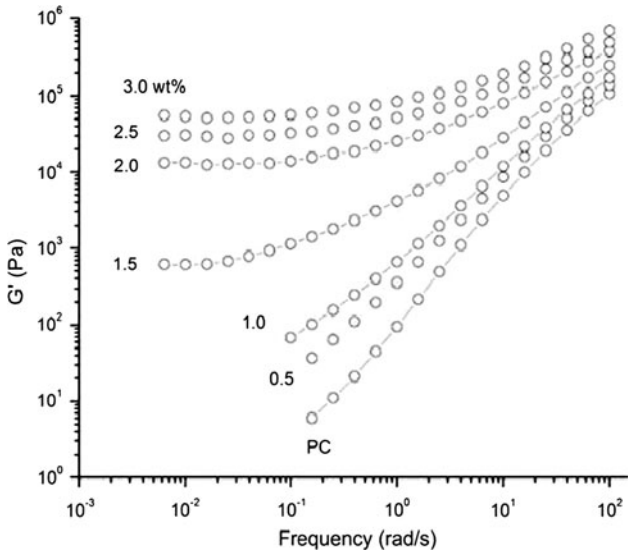


**Fig. 5** Dynamic frequency sweeps of functionalized GNP/polycarbonate (PC) melts after annealing for 10,000 at 230 °C [53]

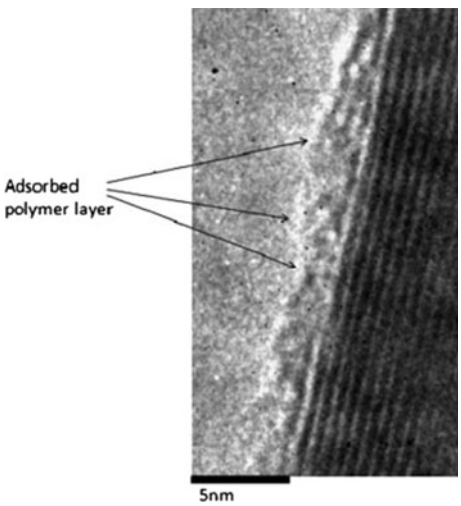


**Fig. 6** TEM microphotographs showing adherence of polymer chains to nanographite surfaces [66]

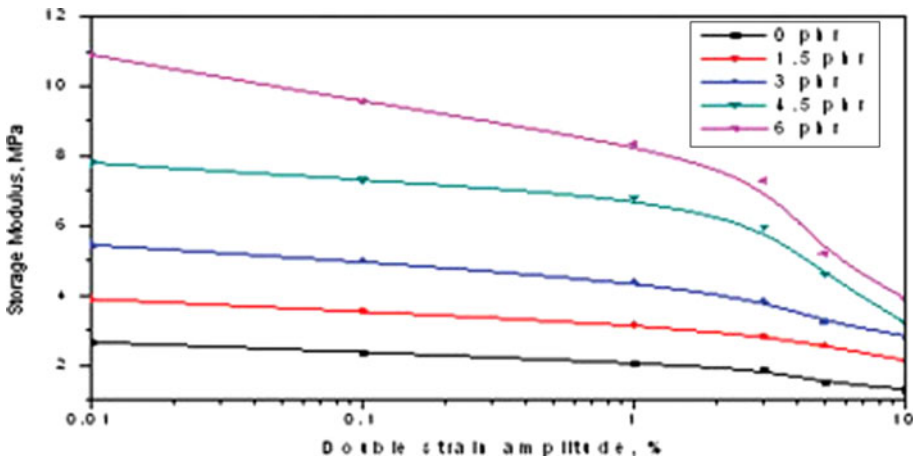


**Fig. 7** Effect of dynamic strain amplitude on storage modulus as a function of filler loading in GNP reinforced flouroelastomers at 50 °C [66]

can increase the number of GNP particles at a given loading, and consequently increase the surface area and effective interfacial bonding, while the GNP networks build up at a low loading level. Thus, it is believed that homogeneously dispersed and highly exfoliated GNPs will always lead to an impressive increase in storage modulus of polymer/GNP nanocomposites. In a similar way, these factors also lead to an increase in loss modulus as well as glass transition temperature ($T_g$).

However, unlike the monotonic increase of storage modulus with the addition of GNPs, the dynamic loss and $T_g$ determined by the relaxation peak on tan ($\delta$) curve (or, sometimes, loss modulus curve) show a more complex dependence on loadings of GNPs. In a study of phenylethynyl-terminated polyimide (PETI)/GNP nanocomposites, three types of GNPs were fabricated to reinforce PETI by ball milling, ultrasonication, and vibratory ball milling, named after EGB, EGU, and EGV, in turn. The size of these GNPs follows the order: EGV < EGU < EGB. The results revealed that PETI reinforced with EGV with smallest particle size and best dispersion show the most dramatic improvement in storage modulus. While, as for $T_g$, in PETI/EGU nanocomposites, it did not always increase with the filler loading. The $T_g$ decreased with the increasing loading of EGU from 5 to 10 wt%, due to a reduced dispersion at high loading of relatively large graphite particles, according to Cho et al. [8]. In another study of PMMA filled with as-received graphite (ARG), expanded graphite (EG) and graphite nanoplatelets (GNP), respectively, the highest reinforcing efficiency was found in GNP-filled PMMA composites, with GNP having a smallest size and largest surface area among three nanofillers. The decrease of $T_g$ at higher loading (5 wt%) was observed in ARG and EG-filled PMMA composites, as a result of poor dispersion, large particle size, small surface area, and weak interface, which did not exist in PMMA/GNP composites [20]. As an indicator of damping properties of polymer nanocomposites, on the tan ($\delta$) curve, the area under the relaxation peak of glass transition usually decreases with the addition of GNPs, owing to the 2D confinement of polymer chain mobility, such as nitrile-butadiene rubber (NBR)-graphite nanocomposites [39] and fluoroelastomer-graphite nanocomposites [67], however, increasing this area has also been observed in epoxy [7, 68]- and vinyl ester [69]-based graphite nanocomposites, reflecting more energy consumption introduced by GNPs.

The contribution of GNPs network to the storage modulus can be verified by measuring the storage modulus as a function of strain amplitude, as shown in Fig. 7. With an increasing strain, the storage modulus goes down slightly for pure polymer and composites at low loading levels; while at high loading level, the amplitude of decreasing of storage modulus becomes larger, especially, at high strains. This can be explained as follows: first, the low concentration of GNPs in polymer matrix could not form an effective network through the composites; second, high strain could significantly change/damage the continuous network structures of GNPs, leading to the decreased storage modulus, while at low strain, the mechanically stable network could exist and bear the strain [64, 70].

## Mechanical properties

Strength, modulus, and toughness of polymer nanocomposites are vitally related to the dispersion quality and interface bonding between polymer matrix and nanofillers. A uniform dispersion and strong interface bonding can benefit the load transfer within the composites. However, in multiple phase composites, the heterogeneity of microstructures of polymer composites also creates many structural flaws (stress concentrations) which are harmful to the mechanical performance. These two competitive aspects lead to different concentration dependencies of mechanical properties. Most studies revealed that the modulus of

polymers could increase with the addition of GNPs, which could be well understood in "Viscoelastic properties." For the strength (tensile strength, flexural strength, tear strength, and compressive strength) and elastic modulus, three types of reinforcing effects by GNPs have been frequently observed: (1) strength goes down with increasing loading [39, 43, 44, 67, 68, 71–75]; (2) strength goes up with increasing loading [44, 54]; (3) strength goes up to a peak value at a critical concentration, and then goes down with further loading [5, 10, 69, 76]. The third situation is usually considered as the ineffective dispersion at higher loading of GNPs, which causes more stress concentration sites and weak interface. On the other hand, the toughness of polymer/GNP nanocomposites seems to be a more challenging task. So far, very little work has succeeded in improving the impact toughness of polymer/GNP nanocomposites at certain loading levels [2, 5, 7, 77], while the deterioration of impact toughness of pure polymer matrix is more frequently reported [54, 56, 59, 73, 78] with the addition of GNPs, although the increasing loading sometimes could improve the toughness (still lower than pure polymer) [78]. Another indicator of the toughness and ductility of polymeric materials, the strain at break, also commonly decreases with the addition of GNPs in polymer matrix [39, 76, 78].

In order to improve the mechanical performance of polymer/GNP composites, great efforts have been made by developing more efficient fabrication methods to improve the dispersion and intercalation of polymer chains into multilayer structures [79], both of which are well-accepted as the most critical factors impacting on the mechanical performances of polymer/2D nanofillers with multilayer structures. For example, it was revealed that the solid-state shear pulverization approach could effectively improve the dispersion and exfoliation of GNPs in polypropylene, which led to the remarkable improvement of Young's modulus (~44%) and elongation at break (~70 times) [56], compared with direct mixing, while a latex compounding technique [34] showed the obvious reinforcement effect on both tensile strength (~103%) and modulus (~6 times)of nitrile-butadiene rubber/GNP composites as a result of improved dispersion. Via a master batch filling technique [54], the tensile strength of HDPE/GNP composites also increased (~14%), due to better dispersion quality. However, similar to direct mixing, all these approaches failed in improving toughness, which was still lower than pure polymers. The effect of different screw systems on microstructures and mechanical properties of LLDPE/GNPs nanocomposites has also been studied [74], revealing the best efficiency of counter-rotation two screw on the tensile strength. UV treatment also proved to be effective in improving the flexural strength of Epoxy/GNP composites [64].

It is not surprising that GNPs have much better reinforcing effect than natural graphite and other larger graphite fillers [2, 6], due to the better dispersion aptitude, more intercalation, and stronger interface bonding. It has been suggested that the deformability or flexibility of the sheet nanoparticles contributes to nanocomposite strength and toughness by reducing the relative value of the Poisson ratio of the composite [80]. A recent study conducted by our group [68] showed a comprehensive improvement in flexural strength, modulus, and fracture toughness of epoxy/GNP composites, in which GNPs were obtained by ball milling, as given in Table 1. Thus, it is reasonable to expect better mechanical properties of GNP-modified polymer nanocomposite, compared with other fillers. Figure 8 gives the flexural modulus of PP/GNP nanocomposites [71]. Obviously, the xGnP-1 (GNP with diameter of 1 μm)-filled PP composites have the highest modulus, indicating the best reinforcement, compared with other fillers. However, for tensile modulus, the PAN-based carbon fiber showed better reinforcement effect than GNP, due to higher degree of fiber orientation along flow direction in the tensile specimen. At the same time, the large GNPs (xGnP-15) with the diameter around 15 μm did not do as well as xGnP-1, reflecting the size dependence. This size dependence resulted from the fact of greater aggregation of larger GNPs (xGnP-15) in the PP matrix, which were more flexible and tended to bend/buckle or become rolled-up, compared with smaller GNPs(xGnP-1). The similar size dependence of flexural strength and impact strength has also been observed in HDPE/GNP composites [73]. In comparative studies of mechanical properties of polyetherimide (PEI)/graphitic nanofillers (MWCNT, CNF, and GNP) revealed that GNP reinforced PEI nanocomposites had the highest strength and modulus compared with the other two. However, the elongation at break of PEI/EG(GNP) nanocomposite was the worst among three types of nanocomposites [72]. Figure 9 presents the comparison of the impact toughness (strength) between HDPE/GNP composites and HDPE/CB composites [5]. Undoubtedly, GNP has a much better toughening effect than CB. In particular, when the concentration of

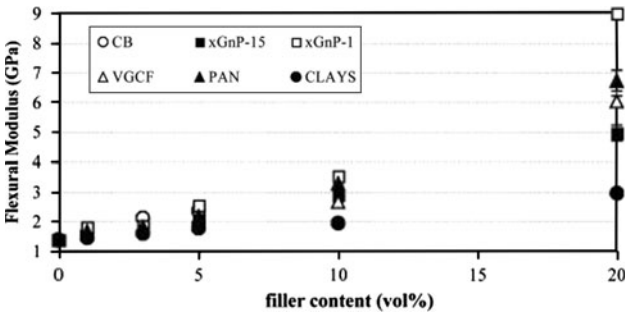


**Fig. 8** Flexural modulus of various PP composites up to filler content of 20 vol.% [71]

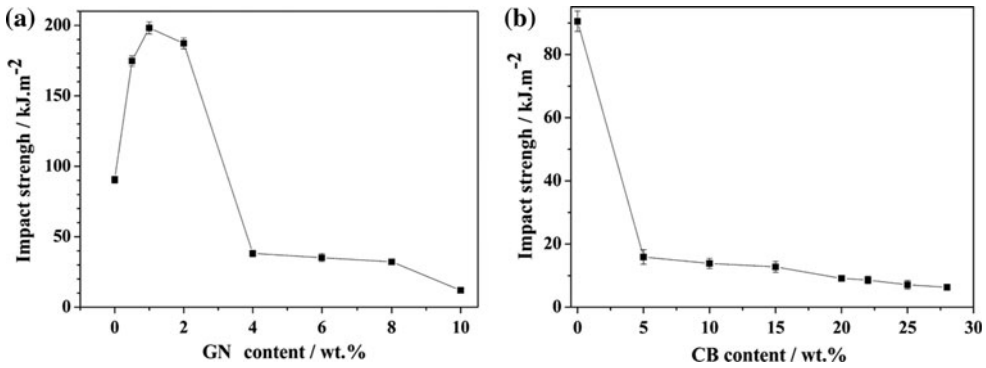


**Fig. 9** Impact strength: **a** HDPE/graphite nanoplatelet (GNP) nanocomposites; **b** HDPE/carbon black (CB) nanocomposites [5]

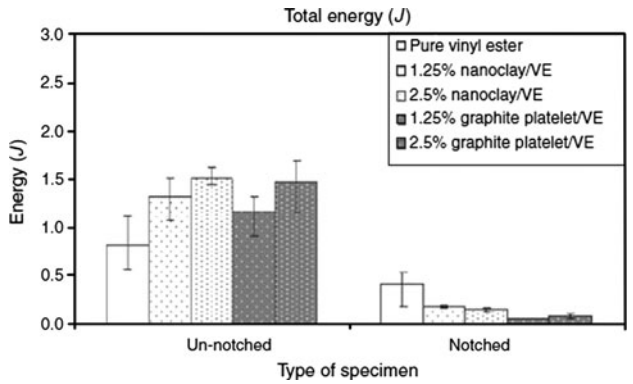


**Fig. 10** Total energy for notched and un-notched pure vinyl ester and nanoclay and graphite platelets reinforced nanocomposites [48]

GNP is smaller than 4% in this study, the impact toughness is several times higher than pure HDPE ( $\sim$90 kJ/m$^2$) with a peak value close to 200 kJ/m$^2$

Another popular 2D nanofiller is nanoclay showing a multilayer structure similar to GNPs. A study of epoxy/GNP nanocomposites [48] showed that the GNP-filled composites have higher elastic modulus than nanoclay nanocomposites. The same results have also been found in vinyl ester nanocomposites [7]. In the same study, the toughness of two vinyl ester nanocomposites filled with nanoclay and GNPs, respectively, has obviously different notch sensitivity (Fig. 10). The notched specimens of 2.5 wt% nanoclay reinforced nanocomposites showed a 50% decrease in energy absorption, while 75 wt% decrease for GNP reinforced vinyl ester nanocomposites, due to the different interface conditions.

## Electrical conductivity

As typical graphitic nanofiller with high electrical conductivity, the application of GNPs in conductive polymer nanocomposites has received extensive attention. A series of thermoplastics and thermosets have been modified by GNPs to improve the electrical properties (NB: electrical conductivity ($\sigma$) = 1/resistivity ($\rho$)), including low electrical percolation threshold and high level-off electrical conductivity after percolation, as summarized in Table 2. Obviously, the polymer/GNP nanocomposites fabricated by "wet" methods, such as in situ polymerization and solution mixing with the assistance of ultrasonication, usually have a lower percolation threshold, compared with direct melt compounding. This should be ascribed to the better dispersion quality and higher degree of exfoliation of GNPs in polymer/GNP nanocomposites fabricated by these "wet" methods, as introduced in "Fabrication of polymer/GNP nanocomposites." However, the level-off electrical conductivity after percolation does not show much difference. Most polymer/GNP nanocomposites level off around $10^{-4}$ to $10^{-3}$ S/cm, regardless of the concentrations of GNPs. According to a recent review on polymer/vapor grown carbon nanofiber composites, we notice the fact that carbon nanotube (CNT) reinforced polymer nanocomposites tend to have a dramatically lower electrical percolation threshold. Currently, many polymer/CNT composites have reported a percolation threshold far below 0.1 vol.% filler loading [88]. This is a percolation level rarely found in GNP/polymer nanocomposites.

High aspect ratio is considered an important structural parameter of GNPs, which is also expected to lead to better electrical properties of polymer/GNP nanocomposites, because the fillers with high aspect ratio can rapidly form conductive networks throughout the composites [89]. But for 2D structured GNP, rather than the aspect ratio, the number of GNP particles also plays a pronounced role in the percolation behavior of polymer/GNP nanocomposites, as revealed by the Drzal's group, finding lower percolation thresholds of polymer nanocomposites filled with GNPs with low aspect ratio (more GNP particles) [4, 90]. The significance of the number of GNP sheets could also be used to explain the better electrical properties of polymer/GNP nanocomposites fabricated by "wet" methods. In the solution mixing method and in situ polymerization technique, the monomers and/polymer chains could get into the porous GNPs easily, and results in higher exfoliation degree. With the help of ultrasonication treatment, not only

**Table 2** Electrical properties of polymer/GNP nanocomposites

| Polymer | Dimensions of GNP ($d$ diameter, $t$ thickness) | Pretreatment/fabrication of GNP | Fabrication of nanocomposites | Percolation threshold | Electrical conductivity (S/cm) | References |
|---|---|---|---|---|---|---|
| PP | 1 μm ($d$)<br>10 nm($t$) | | Coating + compression molding | 0.1 vol.% | $\sim 10^{-4}$ at 3.0 vol.% | [4] |
| HDPE | 5 μm ($d$)<br>70 nm($t$) | | Melt mixing | 2.53 vol.% | $\sim 10^{-6}$ at 8 wt.% | [5] |
| HDPE | N/A | | Master batch filling technique | 16 wt.% | $\sim 10^{-4}$ at 25 wt% | [54] |
| HDPE | N/A | Modified by unsaturated polyester resin | Melt mixing | 5.7 wt% | $\sim 10^{-4}$ at 8 wt% | [60] |
| Epoxy | N/A | UV/ozone treatment | Curing + ultrasonication | N/A | $\sim 10^{-5}$ at 2 wt% | [6] |
| | N/A | | Curing + ultrasonication | N/A | $\sim 10^{-6}$ at 2 wt% | [6] |
| Epoxy | 5–10 μm ($d$)<br>10–100 nm ($t$) | Nitric acid treatment | Curing + ultrasonication | <0.5 vol% | $\sim 10^{-4}$ at 4 vol.% | [81] |
| | 5–10 μm ($d$)<br>10–100 nm ($t$) | | Curing + ultrasonication | <2 vol.% | $\sim 10^{-4}$ at 4 vol.% | [81] |
| Epoxy | N/A | Bromination | Curing + ultrasonication | 1 wt% | $\sim 10^{-4}$ at 2 wt% | [74] |
| PVDF | 10 μm ($d$)<br>50 nm ($t$) | | Solution casting + ultrasonication | 2.4 wt% | $\sim 10^{-4}$ at 4 wt% | [9] |
| PVA | N/A | Electrochemically modified | Solution casting + ultrasonication | 6 wt% | $\sim 10^{-7}$ at 7 wt% | [10] |
| CMPVA | N/A | | Solution casting + ultrasonication | 0.8 wt% | $\sim 10^{-6}$ at 4 wt% | [37] |
| PMMA | 10 nm ($t$) | | Solution mixing + precipitation | N/A | $\sim 10^{-4}$ at 5 wt% | [20] |
| PMMA | N/A | Heating graphite oxide at 500 °C for 20 min under $N_2$ | In situ polymerization in the pores of GNPs | N/A | ~60 at 8 wt% | [42] |
| PMMA | N/A | Graphite oxide | In situ polymerization | ~2 wt% | $\sim 10^{-4}$ at 8 wt% | [82] |
| LLDPE | 15 μm ($d$)<br>10 nm ($t$) | Paraffin coating | Solution mixing (master batch) + melt compounding | N/A | $\sim 10^{-4}$ (GNP:paraffin:LLDPE = 10:10:80) | [72] |
| LLDPE | 15 μm ($d$)<br>5–10 nm ($t$) | Microwave radiation | Solution mixing (master batch) + injection molding | 12–15 wt% | $\sim 10^{-7}$ at 20 wt% | [78] |
| Acrylonitrile-styrene copolymer | N/A | | Master batch filling technique | 9 wt% | $\sim 10^{-3}$ at 15 wt% | [55] |
| PLA | N/A | | Melt mixing | 3–5 wt% | $\sim 10^{-7}$ at 7 wt% | [76] |
| Conjugated PAN | 46 μm ($d$)<br>4.5 nm ($t$) | | Solution casting + ultrasonication | 3–4 wt% | $\sim 10^{-3}$ at 6 wt% | [83] |
| PEN | 485 nm ($d$)<br>36 nm ($t$) | Graphite oxide | Melt compounding | 0.3 vol.% (surface resistance) | – | [49] |
| TPV(PE/EPDM) | N/A | PP-g-MA/GNP master batch | Melt compounding | 6 phr | $\sim 10^{-4}$ at 15 wt% | [51] |

**Table 2** continued

| Polymer | Dimensions of GNP ($d$ diameter, $t$ thickness) | Pretreatment/fabrication of GNP | Fabrication of nanocomposites | Percolation threshold | Electrical conductivity (S/cm) | References |
|---|---|---|---|---|---|---|
| PS | 5–10 μm ($d$)<br>80–150 nm ($t$) | | In situ polymerization | 0.011 vol.% | $\sim 10^{-3}$ at 0.03 vol% | [84] |
| Unsaturated polyester resin | N/A | | In situ polymerization + ultrasonication | 0.64 vol.% | – | |
| Nylon-6 | 13.5 μm ($d$)<br>515 nm ($t$) | | In situ polymerization + ultrasonication | 0.75 vol.% | $\sim 10^{-3}$ at 3 wt% | [85] |
| PODBS | >500 nm ($d$)<br>10–40 nm ($t$) | Microwave radiation followed by ultrasonication | In situ melt polymerization | 4 wt% | $\sim 10^{-3}$ at 5 wt% | [86] |
| PANI | 0.5 μm ($d$)<br>30–100 nm ($t$) | Microwave radiation followed by ultrasonication | In situ polymerization | 1.5 wt% | 33.3 at 1.3 wt% | [87] |
| Silicone rubber | 0.5–20 μm ($d$)<br>30–80 nm($t$) | | Wet mixing + curing | 0.9 vol.% | $\sim 10^{-5}$ at 2 vol% | [39] |

can the dispersion quality be improved, but also the number of exfoliated GNPs will increase. Consequently, the conductive network can be formed at a lower loading level.

The further modification of electrical properties of polymer/GNP nanocomposites can mainly be accomplished in two ways: (1) improve the composites fabrication technique to obtain a better dispersion and exfoliation degree; (2) doping/modification of GNPs. Figure 11 compares the percolation behavior of HDPE/GNP nanocomposites fabricated by direct melt mixing and master batch filling technique. In the master batch filling technique, two master batches were used: PE/GNP and PS/GNP master batches. The results show that the master batch filling technique remarkably decreases the percolation threshold. However, the level-off conductivity of the composites prepared by master batch filling technique is 2–3 orders lower than the composites prepared by direct mixing. It is believed that the encapsulation of GNP sheets by PE and PS inhibited the effective contact among GNP sheets and consequently weakened the tunneling conduction [54]. A coating method developed by Drazl's group [4] proved to be more effective in improving electrical properties, showing the lowest percolation threshold and highest level-off conductivity, compared with traditional solution and melt processing techniques.

Doping modification of GNPs is another commonly used approach to improve the electrical properties of polymer/GNP nanocomposites, primarily via increasing the electrical conductivity of GNP itself. By intercalating proper dopants between graphene planes within the GNPs could effectively increase the conductivity of GNPs, by adding electrons to conduction band or holes to the valence band, and forming charge–transfer complex [74, 83]. Bromine is an ideal dopant of this kind with low toxicity, high stability ease of intercalation, and intermediate chemistry activities. The epoxy nanocomposites with 2 wt% loading GNP showed an approximate two orders increment in electrical conductivity from $\sim 10^{-6}$ to $\sim 10^{-4}$ S/cm. However, the percolation threshold of the nanocomposites before and after bromination did not show any changes [74]. The similar results were also observed in polyacrylonitrile (PAN)/GNP nanocomposites. With the bromine doping, there was no obvious change of percolation threshold, but ca. two orders improvement of level-off conductivity. In the same study, conjugated-PAN was studied as an alternative matrix, due to the ability of conjugated structure to form charge-transfer with $sp^2$ carbons on GNP surfaces by $\pi$–$\pi$ interaction. The conjugated PAN accounts for an impressive four orders increase of level-off conductivity, while having little impact on the percolation threshold (Fig. 12). This conduction mechanism of this composite system combines percolation behavior of GNP and a semiconductive–conductive transition in the conjugated PAN through the doping effect of GNP [83].

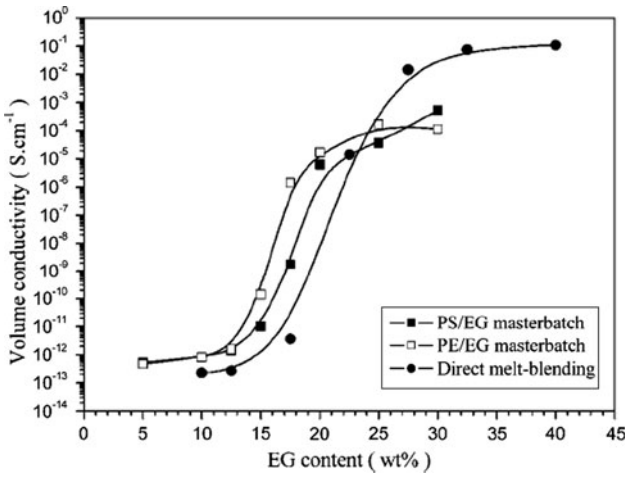


**Fig. 11** Electrical properties of HDPE/GNP nanocomposites prepared by direct melt-extrusion and master batch process [54]

The charge–transfer complex formed by conjugated PANI intercalating into GNPs also led to an increase of electrical conductivity from 5 to 25 S/cm of PANI/GN composites at a rather low loading level of GNP (0.025 wt%) [91]. In another study of PANI/GNP nanocomposites, the conductivity goes up to ~33 S/cm at 1.5 wt% nanographite loading [87]. Silver plating GNP was synthesized to further improve the conductivity of pristine GNP. The resulting conductivity of epoxy composite adhesive is given in Fig. 13. Just like the bromine-doped GNP composites, the silver plating does not change the double percolation behavior of epoxy/pristine–GNP composites, but could effectively increase the electrical conductivity, especially at high loading levels after the second percolation.

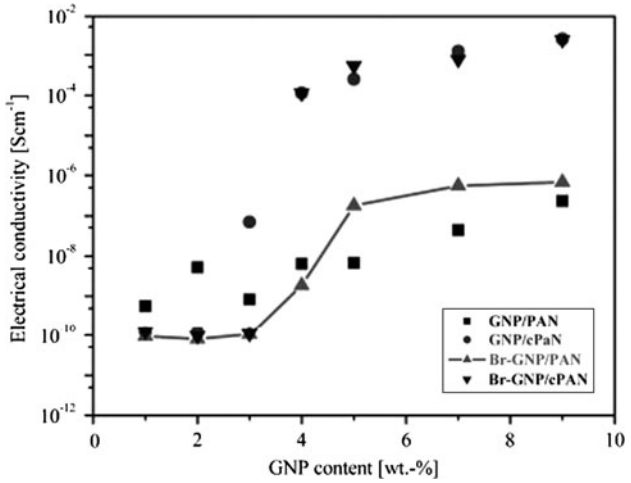


**Fig. 12** The electrical conductivity of the nanocomposite systems as a function of GNP content [83]

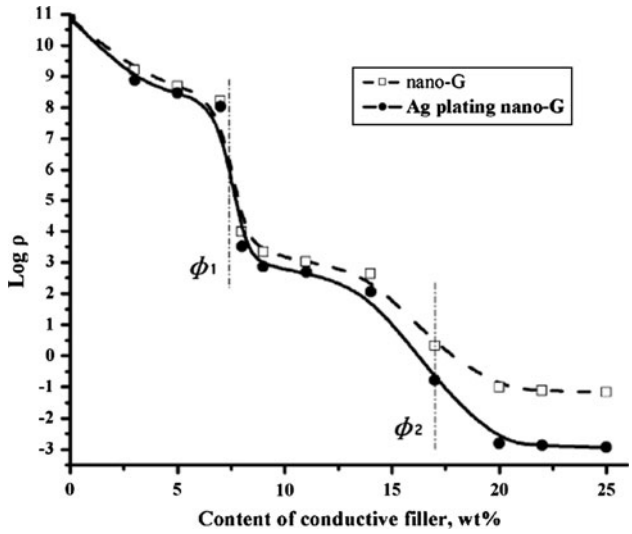


**Fig. 13** Relationship between log resistivity ($\rho$) and the content of conductive filler [92]

Besides traditional bulk polymer/GNP composites, the GNPs potentially could also form many hierarchical structures with various polymers, resulting in excellent functionalities. In particular, owing to the 2D nature of GNPs, they are especially well suited for forming multilayer (layer-by-layer) nanostructures. As shown in Fig. 14 [93], a highly conductive multilayer structure composed of alternating poly(sodium styrenesulfonate) (PSS) and GNP layers was fabricated to achieve an excellent electrical conductivity in the range of 50–200 S/cm, with the bi-layer number ($n$) more than 4.

The temperature, pressure, and chemical dependence of electrical conductivity of polymer nanocomposites hold great promise in fabricating smart materials and sensors with sensitivity to variations of both parameters. Temperature dependence of electrical resistance of carboxymethyl polyvinyl alcohol (CMPVA)/GNP composites was given in Fig. 15 [37]. Unlike traditional positive temperature coefficient (PTC) effect, the peak resistance was observed

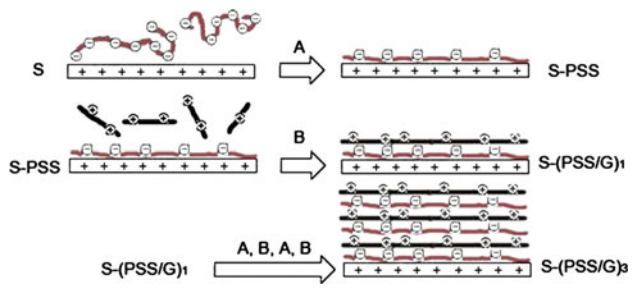


**Fig. 14** The self-assembly process of (PSS/G)n multilayer films. Step A is the deposition of PSS layer; step B is the deposition of C16TAB modified graphite nanoplatelets; by repeating A and B (PSS/G)n multilayer films are obtained [93]

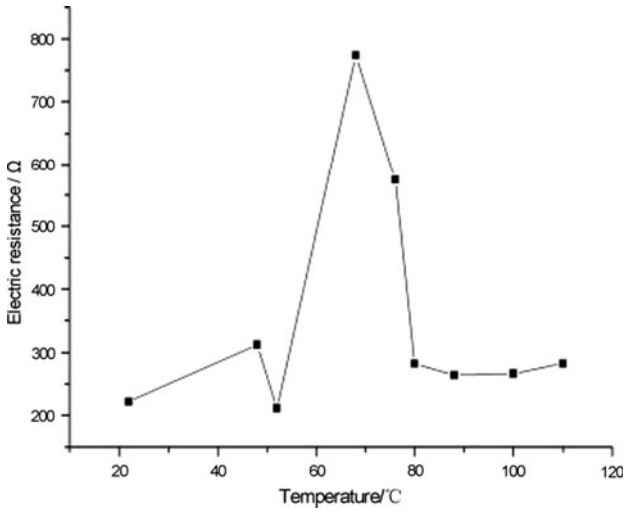


**Fig. 15** The relationship of electrical resistance versus temperature for composites with 3% GNPs [37]

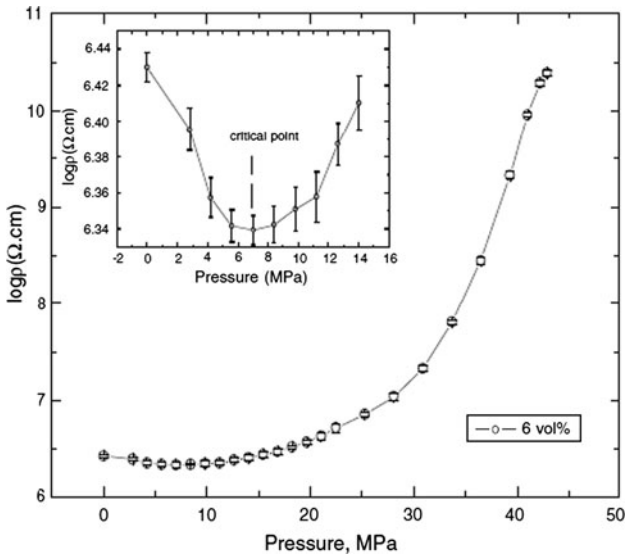


**Fig. 16** Resistivity of HDPE/GNP composite perpendicular to the oriented direction of GNPs as a function of applied pressure [94]

around 70 °C, while after the peak, the resistivity goes back to the original level, a typical negative temperature coefficient (NTC) effect. Two reasons were given in this study to explain this unusual phenomenon:

First, thermal expansion of CMPVA increased the distance among GNP particles and destroyed the conducting network. Second, thermal disturbance of conducting charges activated electron hopping and increased the electrical conductivity [37]. Similar PTC and NTC effects have also been observed in epoxy/GNP composites at percolation threshold. Chen et al. [45, 94, 95] did comprehensive studies on the piezoresistivity behavior of HDPE/GNP nanocomposites and silicone rubber/GNP nanocomposites. A typical pressure–resistivity relationship is shown in Fig. 16. The variation of electrical resistivity reflects the construction and deconstruction of conductive network under different pressures. The initial decrease of electrical resistivity indicates that a more effective conductive network has been developed under low pressure. With further increase of pressure, the deconstruction of conductive network happens, leads to the rapid increase of resistivity. The critical pressure as indicated in Fig. 16 increases with graphite loading [94]. Owing to the large basal spacing, more polar groups and porous structures of GNPs, the diffusion and absorption of organic molecules will be favored. Figure 17 shows resistance sensitivity of poly (methyl acrylic acid) (PMAA)/GNP nanocomposites and PMAA to the vapors of different organic solvents. In particular, PMAA/GNP nanocomposites have the strongest sensitivity to chloroform vapor, with a huge increase of resistance as a result of weaken mutual effects among graphite nanosheets, indicating the destroyed conductive network after absorption of chloroform, while the exposure to acetone vapor has almost no effect on the electrical properties of the nanocomposites [96].

## Dielectric properties

Dielectric constant, or relative permittivity, reflects the ability of materials to store electrical energy. For pure polymers, the dielectric constant is usually between 2 and 10. Except for the applications in high-speed integrated circuit and fast static dissipation, which calls for a low dielectric constant, high dielectric constant is usually

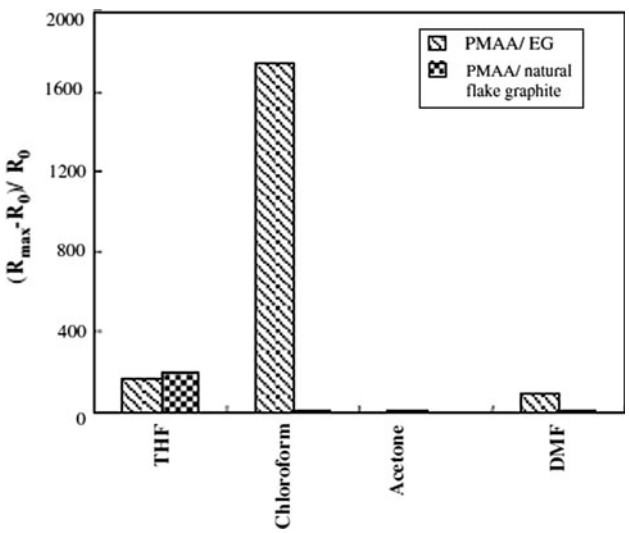


**Fig. 17** Electrical resistance response intensities ($(R_{max} - R_0)/R_0$) of **a** PMAA/natural flake graphite composites and **b** PMAA/GNP (EG nanoparticles) nanocomposites thin films to various solvent vapors [96]

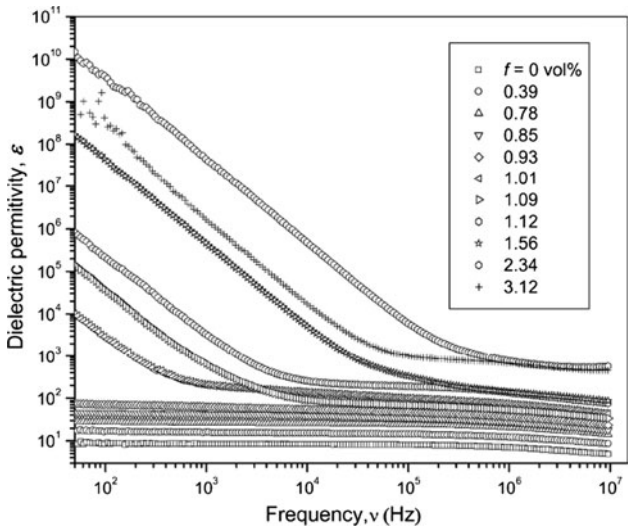


**Fig. 18** Dependence of dielectric constants on the frequency for PVDF/GNP nanocomposites at room temperature [97]

expected. By introducing conductive fillers into a polymer matrix, a high dielectric constant could be realized through interfacial polarization mechanism (Maxwell–Wagner–Sillars polarization (MWS)). As for GNPs, their high surface area as a result of the 2D structure could create more interface area compared with other nanofillers, and more charges will be expected to be trapped at the interface, thus, GNPs show great potential in fabricating polymer/GNP nanocomposites with high dielectric constant, due to stronger interfacial polarization. So far, the highest dielectric constant reported for GNP-filled polymer nanocomposites was in poly(vinylidene fluoride) (PVDF)/GNP composites fabricated by solution–cast method and compression molding, as shown in Fig. 18 [97]. At 1000 Hz, the dielectric constant of PVDF/GNP nanocomposites gets close to $10^8$ at a rather low loading level (2.34 vol.%), and even at high frequencies, such as 1000 kHz, the dielectric constant still remains high at around 1000. The homogeneous dispersion of GNPs in PVDF was considered the main structural factors leading to such a high dielectric level. Some other improvements of dielectric constant caused by well-dispersed GNPs includes ca. 5000 at 1000 Hz in PVDF nanocomposites (4 wt%) [9]; ca. 500 at 1000 Hz in polystyrene nanocomposites (3.1 vol.%) [84], ca. 250 at 1000 Hz in epoxy nanocomposites (5.0 wt%) [64], 10 at 1 GHz (5 vol.%) in epoxy nanocomposites [81]. The dielectric constant usually exhibits a percolation behavior in polymer/GNP nanocomposites, following the same power law (Eq. 5) as electrical conductivity does [9]. In Fig. 18, the PVDF/GNP nanocomposites have a dielectric percolation threshold around $\phi_c = 1.01$ vol.%. Above this threshold, the dielectric constant shows a significant increase, especially at low frequencies. Furthermore, the strong frequency dependence of the dielectric constant reveals the fact of strengthened interface polarization.

$$\varepsilon'(f) \propto \left|\frac{\phi_c - \phi}{\phi_c}\right|^{-s} \quad (5)$$

As discussed in previous sections, the degree of exfoliation of GNPs is critical to the properties of polymer nanocomposites, generally in a good way. For the dielectric constant, the same relationships also exist. To increase the exfoliation degree is equivalent to increasing the effective surfaces which could contact with polymer matrix and create more interface area, thus, it is reasonable to expect an extremely high dielectric constant in polymer/GNP nanocomposites with high exfoliation degree, although there are no comprehensive and comparative studies on this subject. On the other hand, according to the "mini capacitor" concept, frequently used for explaining high dielectric constant in polymer/graphitic nanofiller composites, the high exfoliation degree, and more intercalation of polymers into the GNPs leads to an increasing number of mini (nano) capacitors, and consequently high dielectric constant.

Dielectric loss, as another important aspect, is gaining increasing attention today, and materials with high dielectric constant and low dielectric loss are in urgent demand. Dielectric loss represents the energy consumption during the alignment and orientation of dipoles with external electric field. The more aligned and oriented dipoles, on one hand, accounts for the improvement of dielectric constant; on the other hand, also lead to higher dielectric loss, as shown in Fig. 19. Thus, it is still a challenging task to increase the dielectric constant while maintaining the loss at a relatively low level. Although some work has been done on metal nanofillers, carbon nanofibers and carbon nanotubes-filled nanocomposites by introducing multilayer structures and insulating gaps between polymer matrix and conductive fillers [98–101],

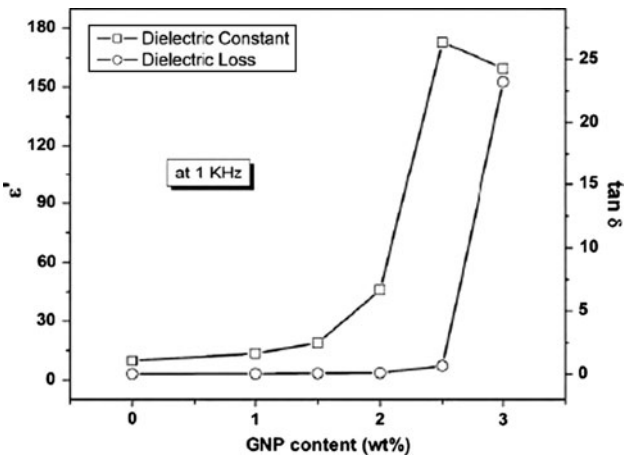


**Fig. 19** Dielectric constant and dielectric loss as a function of GNP content for PVDF/GNP composites [9]

there is no effort made to GNP-filled polymer nanocomposites system currently. The temperature dependence of dielectric properties, particularly, dielectric loss, could be used to study the relaxation mechanisms of composites systems. With increasing temperature, the mobility of polymer chains and dipoles will get easier. On one hand, more dipoles could form and orient as a response to electric field, on the other hand, owing to the high kinetic energy of dipoles at high temperature, the alignment and orientation of dipoles along the electric field become more difficult. These two competing aspects make the temperature dependence of polymer/GNP nanocomposite truly complicated. Also, taking the relaxation of polymer matrix with temperature into consideration (such as glass transition) both dielectric constant and dielectric loss are possible to go up, down, or keep constant over a wide temperature range, revealing the multiple possible interactions among polymer matrix and GNP particles. Therefore, similar to DMA, dielectric relaxation is very useful in understanding structures and properties of polymer/GNP nanocomposites [9, 69, 102].

## Thermal conductivity and thermal stability

Thermal conductivity is primarily determined by the vibration of lattice phonons, and also by thermal motion of electrons [64]. However, currently, the understanding on the thermal conduction mechanisms of polymer nanocomposite is still insufficient, especially on the lattice vibration behavior. Due to the high thermal conductivity of GNPs, the incorporation of GNPs in a polymer matrix generally leads to an increase in thermal conductivity [16, 50, 62, 103]. Factors including the aspect ratio of GNP, interface, and contact resistance show significant influences on the thermal conductivity, in addition to concentration. Figure 20 shows the thermal conductivity of epoxy/10 wt% GNP nanocomposites filled with three GNPs with different aspect ratio. The highest aspect ratio leads to the best thermal conductivity [104]. The same results have also been observed in PP/GNP composites, in which the GNPs with a diameter of 15 μm leads to higher thermal conductivity of the nanocomposites, compared with GNPs having a diameter of 1 μm, owing to a smaller contact resistance of GNPs with high aspect ratio [16]. The study of thermal conductivity of epoxy/GNP nanocomposites suggested the importance of interface thermal resistance on the thermal conductivity of composites. After the GNPs were treated by nitric acid, the interfacial bonding was improved due to the existence of polar groups on the GNPs, so is the interface thermal resistance. Consequently, the thermal conductivity of nitric acid treated GNP (1 vol.%) has better modification efficiency, as given in Fig. 21 [105]. Lastly, dispersion of nanofillers is also important. In ethylene-co-vinyl acetate (EVA)/graphite oxide (GO) nanocomposites, the thermal conductivity decreased at highest loading (4 phr), as a result of aggregation of fillers [44].

The superiority of GNPs as a functional modifier is further reflected by its high efficiency in improving the thermal conductivity of PEI nanocomposites. Compared with CNF and MWCNT, the GNP-filled PEI nanocomposites have the highest thermal conductivity along the direction of nanofiller alignment in a wide loading range, no matter whether solution or melt mixing was applied to prepare the composites (Fig. 22). In the same study, the un-oriented composites have also been prepared, still

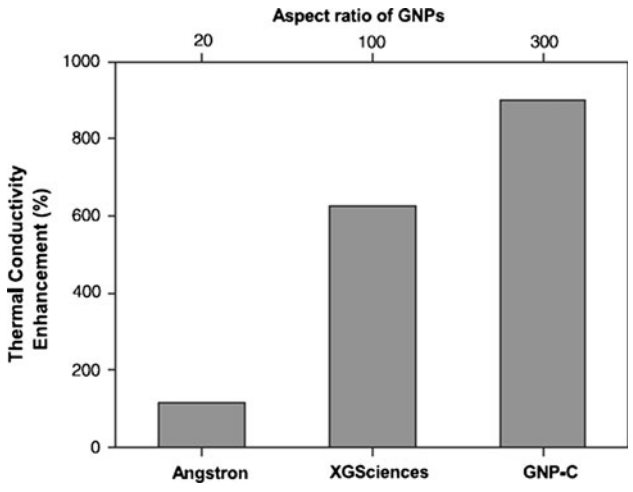


**Fig. 20** Thermal conductivity enhancement of GNP–epoxy composites at 10 wt% of GNP loading for GNP fillers produced by commercial suppliers Angstron Materials LLC and XG Sciences, Inc. in comparison with GNP-C filler [104]

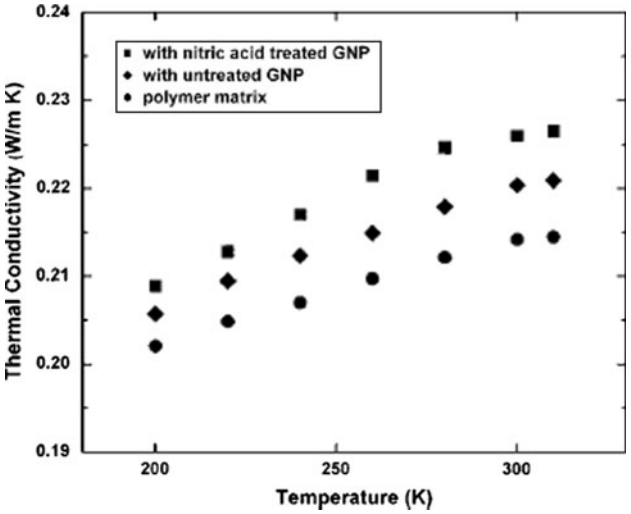


**Fig. 21** The thermal conductivity of polymer composites reinforced with graphite nanoplatelets (GNPs) as a function of temperature [105]

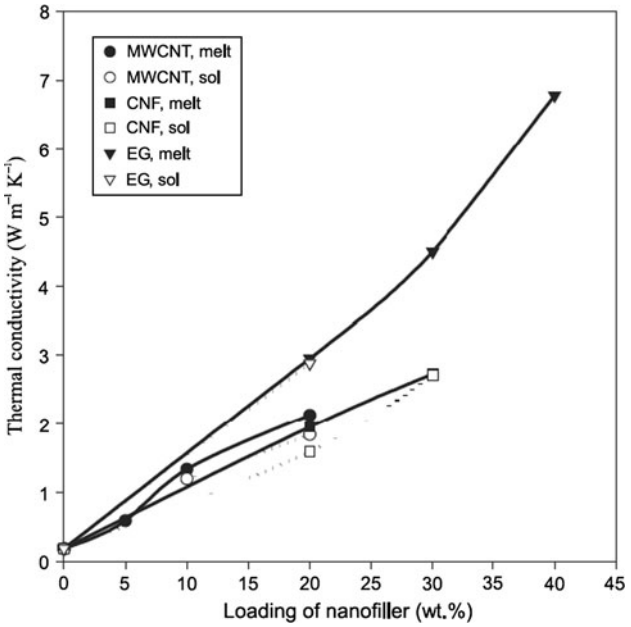


**Fig. 22** Thermal conductivity of molded PEI (UltemTM)/carbon nanofiller samples-measurement along direction of alignment [62]

resulting in the highest thermal conductivity in GNP/PEI nanocomposites.

Thermal stability covers two aspects of chemical stability evaluated by onset temperature ($T_o$) of thermal degradation/decomposition, and physical stability evaluated by the coefficient of thermal expansion (CTE). There is some doubt that the addition of GNPs in polymer matrix could improve both of them. Table 3 summarizes the increasing amplitude of $T_o$ of various polymer/GNP nanocomposites systems.

From Table 2, we can tell that the properties of polymer matrix and graphite fillers are really critical to the improvement of thermal stability. Several mechanisms have been proposed to explain the contribution of GNPs to the improved the thermal stability, here, we list some of them: (1) the homogeneously dispersed GNPs acts as "efficient heat sinks," which extracted more heat than the matrix and did not allow the accumulation of heat within the latter, thereby preventing oxidation at the early stages of degradation [10]; (2) the homogeneously dispersed GNPs could serve as mass transfer barriers (shielding effect) against the volatile pyrolized products [65, 76]; (3) the interfacial polymer phases in the vicinity of the graphite nanoparticle surfaces are restricted by the bonding from GNPs, and the energy needed to decomposition would increase, altering the ability of degraded molecules to diffuse and evaporate [20, 91]. The interface area shows significant importance to the thermal degradation behavior, which could be further reflected by the fact that the thermal stability of LLDPE nanocomposites filled with paraffin-oil-coated GNPs increased with GNP loading. The paraffin oil coating layer with very low thermal stability between LLDPE and GNPs prevents the positive effect GNPs on the thermal stability [72].

Thermal expansion is very common to polymeric materials serving at high temperature. The addition of rigid fillers to polymer matrix is a useful way to restrain the thermal expansion, due to the confinement effect of rigid fillers with low thermal expansion. The results listed in Table 4 reveals that the CTE will increase with temperature, and decrease with higher loading. From the effect of processing on CTE, the composites fabricated via counter twin screw, which showed best dispersion quality and mechanical performances [65] have the best dimension stability, i.e., lowest CTE, indicating a uniform dispersion of GNPs (xGnP) benefiting the dimension stability of polymer nanocomposites. Compared with other 0D and 1D nanofillers, the excellence of GNPs in improving the dimensional stability is obvious, according to Figs. 23 and 24. At temperature below $T_g$, the injection molded sample of PP/GNP composites shows lowest CTE along both

**Table 3** Effect of GNPs on thermal stability

| Polymer | Types of GNPs | Concentration of GNP | Increase of $T_o$ (°C) | References |
|---|---|---|---|---|
| PVA | GNP | 5 wt% | 45 | [10] |
| PMMA | GNP | 5 wt% | 35 | [20] |
| PMMA | As-received graphite | 5 wt% | 20 | [20] |
| PLA | Exfoliated graphite | 3.0 wt% | 14 | [76] |
| PANI | GNP | N/A | 40 | [91] |
| Flouroelastomer | GNP | 7 phr | 7 | [67] |
| PS | GIC-220N | 5 wt% | 80 | [106] |
| HIPS | GIC-220N | 5 wt% | None | [106] |
| ABS | GIC-220 | 5 wt% | 10 | [106] |
| Nylon-6 | Foliated graphite | 5 wt% | 24 | [85] |

**Table 4** The coefficient of thermal expansion (CTE) of GNP(xGnP)/LLDPE nanocomposites by different rotating systems in melt mixing as xGnP different loading contents in the range of 45–80 °C and 85–100 °C [65]

| Temperature range | 45–80 °C | | 85–100 °C | |
|---|---|---|---|---|
| xGnP loading | 5 wt% | 12 wt% | 5 wt% | 12 wt% |
| Screw rotation | | | | |
| Co-rotating | 253.4 | 174.8 | 373.1 | 337.9 |
| Counter-rotating | 245.7 | 173.1 | 340.1 | 285 |
| Modified-Co-rotating | 258.5 | 223.5 | 378.6 | 335 |

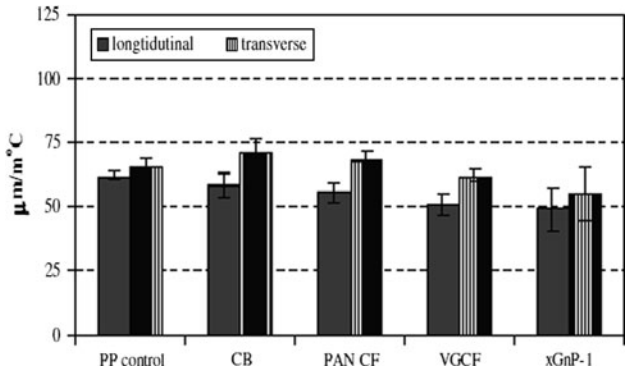


**Fig. 23** CTE of 3 vol.% carbon reinforced PP composites for $T < T_g$ [16]

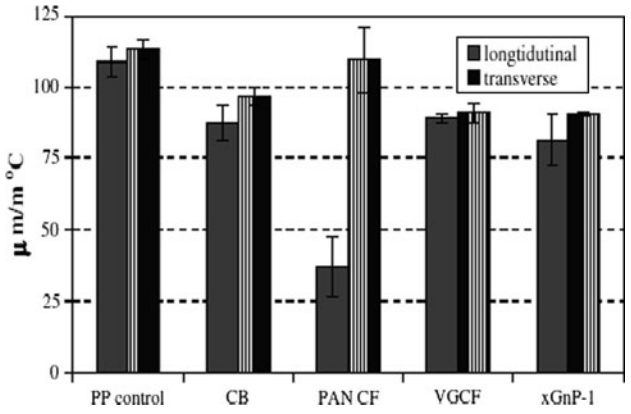


**Fig. 24** CTE of 3 vol.% carbon reinforced PP composites for $T > T_g$ [16]

longitudinal direction and transverse direction. When the temperature is above $T_g$, except for the CTE along longitudinal direction (PAN CF is the best), PP/GNP nanocomposites still possess the best dimensional stability exhibiting a rather low CTE. It is believed that the advantages of GNPs as dimensional stabilizers should be owing also to the 2D multilayer structures of GNPs.

## Synergy of GNP with other carbon nanofillers on polymer nanocomposites

Adding hybrid nanofiller systems containing two or three types of nanofillers to a polymer matrix has proven to be a favorable way to improve the properties of polymer nanocomposites, in particular, the physical properties. The resulting composites usually have much better performances than the composites filled only with individual nanofillers. In the epoxy nanocomposites [107, 108], the synergetic effect of GNPs, with carbon black (CB) and carbon nanotube (CNT) can lead to the formation of excellent conductive networks as shown in Fig. 25(c), which accounts for the highest electrical conductivity of epoxy/GNP-CB-CNT hybrid filler nanocomposites. At the same time, the binary filler system of GNP + CB also showed better reinforcement effects than individual GNPs. The synergetic effect of CNTs and GNPs has also been reported in epoxy nanocomposites [109] and polyethermide (PEI) nanocomposites [110], revealing the dramatically increased electrical conductivity at low loading levels compared with GNP-filled nanocomposites and CNT-filled nanocomposites. In the PEI nanocomposites [110], the synergy of CNT and GNP has also been reflected by the higher thermal conductivity of PEI/(CNT + GNP) composites, owing to the uniform dispersion and formation of effective networks between CNTs and GNPs, as shown in Fig. 26. In [109], the flexural properties of epxoy/CNT/GNP (CNT + GNP = 2.0 wt%) hybrid composites have also been studied, however, there was no synergy effect observed, unlike with the electrical properties. This is probably because the electrical properties mainly rely on the networks of nanofillers in the polymer matrix, which is sensitive to the variation of the ratio of GNP and CNT, while the mechanical properties are more dependent on the dispersion and interfacial bonding between polymer and nanofillers. Thus, at a fixed total amount of GNP and CNT, the flexural properties did not show obvious changes, assuming similar interfacial bonding between nanofillers and polymers. However, due to the lack of studies of hybrid nanocomposites containing GNPs, it is still too early to conclude that there is no synergy effect of GNP and other carbon nanofillers on mechanical properties without comprehensive studies.

## Conclusion and perspective

The graphite nanoplatelet (GNP) has already proven itself to be a powerful solid modifier for improving the properties of polymers and fabricating high-performance polymer nanocomposites. Their 2D graphitic structures with high surface area account for larger interface area and more

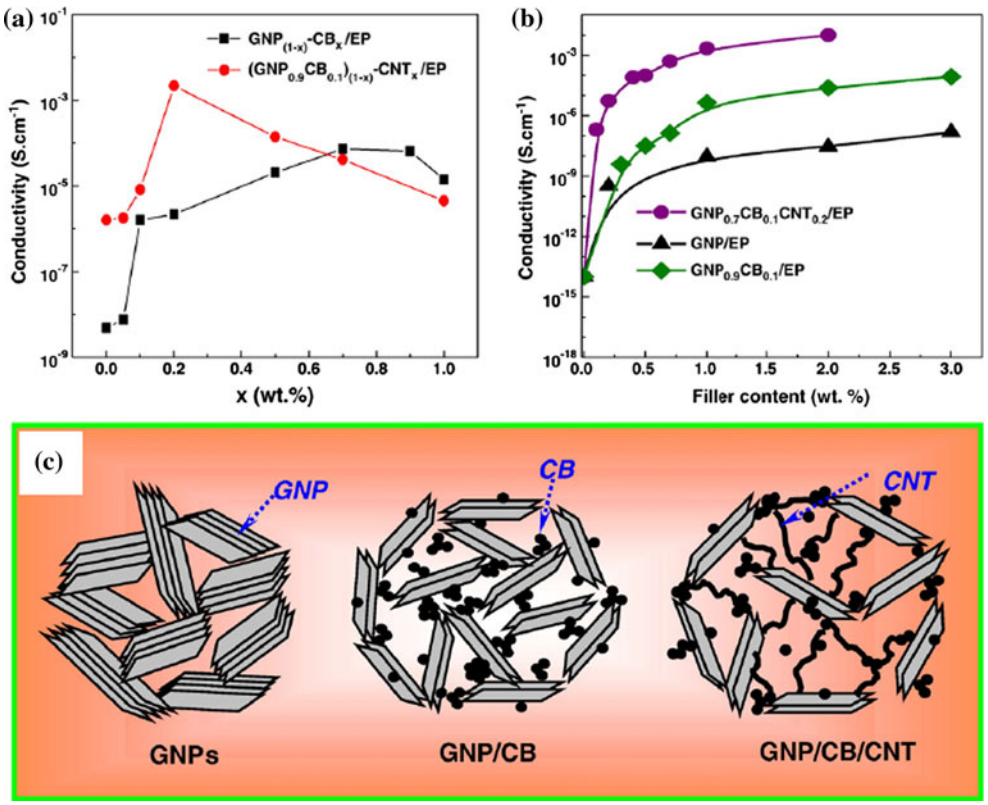


**Fig. 25** The variation of the electrical conductivity of the composite as a function of weight ratios of CB/(GNP + CB) and CNT/(GNP + CB + CNT) (total filler content is 1 wt%) (**a**) and the electrical conductivity of GNPs/EP, $GNP_{0.9}$ $CB_{0.1}$/EP, and $GNP_{0.7}$ $CB_{0.1}$ $CNT_{0.2}$/EP as a function of the filler content (**b**). Schematic illustrations for the synergistic effect among GNPs, CB, and CNTs (**c**) [108]

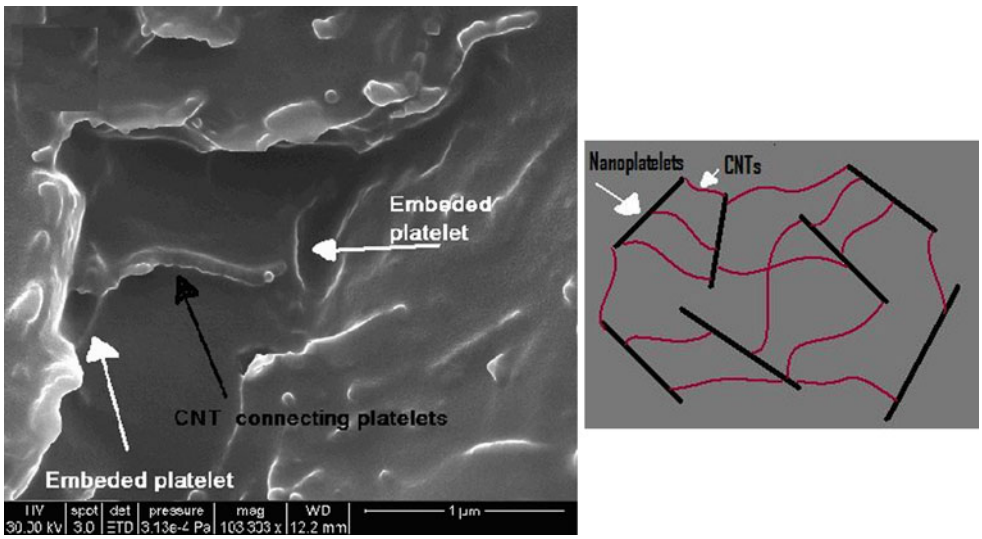


**Fig. 26** FESEM images of 0.5 wt% GNP/MWCNT hybrid composites with equal amounts of GNPs (0.25 wt%) and MWCNTs (0.25 wt%) [110]

interactions between polymers and GNP particles. Correspondingly, they exhibit unique advantages compared with other graphitic carbon nanofillers, thus, in many applications, GNPs have shown much better reinforcement efficiency. Besides the aspect ratio, dispersion quality, the exfoliation degree of GNP is a critical factor exerting significant effects on the performance of polymer/GNP nanocomposites. According to this review, we find that the high exfoliation degree is good for most properties of GNP-filled polymer nanocomposites, similar to other 2D nanostructures, such as nano-clay and nano-silicate. But GNPs are superior to these other 2D nanostructures, since

they not only have excellent mechanical properties, but also have great wear resistance, high electrical, and thermal conductivities. Thus, multifunctionalities can be readily obtained by adding GNPs to a polymer matrix. Correspondingly, to fabricate high-performance polymer/GNP nanocomposites, the structure–property relationships of polymer/GNP nanocomposites need to be fully understood, especially the rheological properties which essentially relate to the processing of polymer nanocomposites, in particular, the dispersion and exfoliation of GNPs in a polymer matrix. In contrast to the fruitful results on other 2D nanoparticle-filled polymer nanocomposites, the relevant research on polymer/GNP nanocomposites is still nascent. Moreover, its 2D nanostructure also makes GNPs an ideal candidate to improve the gas barrier property of polymeric materials, which has not obtained substantial attention yet.

Owing to the extraordinary physical and mechanical properties of monolayer graphene, since the monolayer graphene sheet was successfully fabricated in 2004, studies on manufacturing of fully exfoliated GNPs (i.e., monolayer graphene sheet) have been exploding, especially after the 2010 Nobel Physics Prize was awarded for the fabrication of graphene. Undoubtedly, the development of polymer/monolayer graphene sheet composites is the future of high-performance multifunctional polymer nancomposites, but which is critically dependent on the production of graphene. However, there are many challenges and difficulties in the production of graphene, typically including the extremely low yield and deteriorated properties by commonly used oxidization procedures to fully exfoliate the graphite. Although abundant work on polymer/graphene nanocomposite has been reported, most could not provide direct proof of the monolayer graphene sheets in a polymer matrix. In fact, what they obtained are usually GNPs containing a few graphene layers, but not monolayer graphene sheets. Due to the coupling effect among graphene sheets, the graphite crystal with more than 10 graphene layers starts to behave like bulk graphite. This is probably one reason why the properties of these reported nanocomposites are not as good as expected, and far below theoretical predictions. On the other hand, besides the manufacturing of monolayer graphene sheets, a new challenge to fabrication of polymer/graphene nanocomposites is arising. Due to the extremely high aspect ratio of monolayer graphene sheets, the current processing techniques discussed above may not be capable of avoiding aggregation. The demand for new dispersion techniques is an imperative.

Finally, the favorable opinion of many that polymer/graphene nanocomposites will enable a new generation of high-performance composites is fundamentally based on the extraordinary electronic structure and properties of graphene, however, we cannot evade some exigencies for successful implementation, for example, these attractive properties are also essentially related to imperfections and quality issues such as impurities, surface ripples (quasi-2D) and damaged edges of graphene. Thus, the contributions and limitations on the performance and functionalities of polymer nanocomposites deserve substantial attention in the immediate future.

## References


1. Viculis LM, Mack JJ, Mayer OM, Hahn HT, Kaner RB (2005) J Mater Chem 15:974
2. Pramoda KP, Hussain H, Kou HM, Tan HR, He CB (2010) J Polym Sci A 48:4262
3. Fim F, Guterres JM, Basso NRS, Galland GB (2010) J Polym Sci A 48:692
4. Kalaitzidou K, Fukushima H, Drzal LT (2007) Compos Sci Technol 67:2045
5. Wang L, Hong J, Chen G (2010) Polym Eng Sci 50:2176
6. Li J, Kim JK, Sham ML (2005) Scripta Mater 53:235
7. Gupta S, Mantena PR, Al-Ostaz A (2010) J Reinf Plast Compos 29:2037
8. Cho D, Lee S, Yang G, Fukushima H, Drzal LT (2005) Macromol Mater Eng 290:179
9. Li YC, Tjong SC, Li RKY (2010) Synth Met 160:1912
10. Hu H, Chen G (2010) Polym Compos 31:1770
11. Tibbetts GG, Lake ML, Strong KL, Rice BP (2007) Compos Sci Technol 67:1709
12. Tang QY, Chan YC, Wong NB, Cheung R (2010) Polym Int 59:1240
13. Lu MD, Yang SM (2005) Synth Met 154:73
14. Peng H (2008) J Am Chem Soc 130:42
15. Jordan J, Jacob KI, Tannenbaum R, Sharaf MA, Jasiul I (2005) Mater Sci Eng A 393:1
16. Kalaitzidou K, Fukushima H, Drzal LT (2007) Carbon 45:1446
17. Yakovlev AV, Finaenov AI, Zabud'kov SL, Yakoleva EV (2006) Russ J Appl Chem 79:1741
18. Li J, Lin H, Zhao W, Chen G (2008) J Appl Polym Sci 109:1377
19. Fan H, Wang L, Zhao K, Li N, Shi Z, Ge Z, Jin Z (2010) Biomacromolecules 11:2345
20. Ramanathan T, Stankovich S, Dikin DA, Liu H, Shen H, Nguyen ST, Brinson LC (2007) J Polym Sci B 45:2097
21. Park S, Ruoff RS (2009) Nat Nanotechnol 4:217
22. See CH, Harries AT (2007) Ind Eng Chem Res 46:997
23. Nozaki T, Okazaki K (2008) Plasma Process Polym 5:300
24. Scott CD, Arepalli S, Nikolaev P, Smalley RE (2001) Appl Phys A 72:573
25. Zhan Y, Lei Y, Meng F, Zhong J, Zhao R, Liu X (2011) J Mater Sci 46:824. doi:10.1007/s10853-010-4823-7
26. Wu X, Qi S, He J, Duan G (2010) J Mater Sci 45:483. doi:10.1007/s10853-009-3965-y
27. George JJ, Bhowmick AK (2008) J Mater Sci 43:702. doi:10.1007/s10853-007-2193-6
28. Lu W, Wu D, Wu C, Chen G (2006) J Mater Sci 41:1785. doi:10.1007/s10853-006-3946-3
29. Jang BZ, Zhamu A (2008) J Mater Sci 43:5092. doi:10.1007/s10853-008-2755-2
30. Novoselov KS, Geim AK, Morozov SV, Jiang D, Zhang Y, Dubonos SV, Grigorieva IV, Firsov AA (2004) Science 306:666
31. Kim H, Abdala AA, Macosko CW (2010) Macromolecules 43:6515

32. Stankovich S, Dikin DA, Piner RD, Kohlhaas KA, Kleinhammes A, Jia Y, Wu Y, Nguyen SY, Ruoff RS (2007) Carbon 45:1558
33. Gilje S, Han S, Wang M, Wang KL, Kaner RB (2007) Nano Lett 7:3394
34. McAllister MJ, Li JL, Adamson DH, Schiepp HC, Abdala AA, Jun L, Herrera-Alonso M, Milius DL, Car R, Prudhomme RK, Aksay IA (2007) Chem Mater 19:4396
35. Lotya M, Hernandez Y, King PJ, Smith RJ, Nicolosi V, Karlsson LS, Blighe FM, De S, Wang Z, McGovern IT, Duesberg GS, Goleman JN (2009) J Am Chem Soc 131:3611
36. Bhaviripudi S, Jia XT, Dresselhaus MS, Kong J (2010) Nano Lett 10:4128
37. Yu C, Li B (2008) Polym Compos 29:998
38. Du XS, Xiao M, Meng YZ, Hay AS (2004) Polym Adv Technol 15:320
39. Yang J, Ming T, Jia QX, Shi JH, Zhang LQ, Lim SH, Yu ZZ, Mai YW (2007) Acta Mater 55:6372
40. Mack JJ, Viculis LM, Ali Ashraf, Luoh R, Yang G, Hahn HT, Ko FK, Kaner RB (2005) Adv Mater 17:77
41. Hussain F, Hojjati M, Okamato M, Gorga RE (2006) J Compos Mater 40:1511
42. Wang WP, Liu Y, Li XX, You YZ (2006) J Appl Polym Sci 100:1427
43. Lu J, Drzal LT, Worden RM, Lee I (2007) Chem Mater 19:6240
44. George JJ, Bandyopadhyay A, Bhowmick AK (2008) J Appl Polym Sci 108:1603
45. Chen L, Lu L, Wu D, Chen G (2007) Polym Compos 28:493
46. Wu TL, Lo TS, Kuo WS (2010) Polym Compos 31:292
47. Zhao W, Wang H, Tang H, Chen G (2006) Polymer 47:8401
48. Yasmin A, Luo JJ, Daniel IM (2006) Compos Sci Technol 66:1182
49. Kim H, Macosko CW (2008) Macromolecules 41:3317
50. Planes E, Duchet J, Maazouz A, Gerard JF (2008) Polym Eng Sci 48:723
51. Katbab AA, Hrymak AN, Kasmadjian K (2008) J Appl Polym Sci 107:3425
52. Gopakumar TG, Pagé DJYS (2004) Polym Eng Sci 44:1162
53. Kim H, Macosko CW (2009) Polymer 50:3797
54. Li YC, Chen GH (2007) Polym Eng Sci 47:882
55. Chen G, Chen X, Wang H, Wu D (2007) J Appl Polym Sci 103:3470
56. Wakabayashi K, Pierre C, Dikin DA, Ruoff RS, Ramanathan T, Brinson LC, Torklson JM (2008) Macromolecules 41:1905
57. Furgiuele N, Lebovitz AH, Khait K, Torkelson JM (2000) Macromolecules 33:225
58. Pujari S, Ramanathan T, Kasimatic K, Masuda J, Adnrews R, Torkelson JM, Brinson LC, Burghardt WR (2009) J Polym Sci B 47:1426
59. Wakabayashi K, Brunner PJ, Masuda J, Hewlett SA, Torkelson JM (2010) Polymer 51:5525
60. She Y, Chen G, Wu D (2007) Polym Int 56:679
61. Du XS, Xiao M, Meng YZ, Hay AS (2004) Synth Met 143:129
62. Ghose S, Working DC, Connell JW, Smith JG Jr, Watson KA, Delozier DM, Sun YP, Lin Y (2006) High Perform Polym 18:961
63. Vermant J, Ceccia S, Dolgovskij MK, Maffettone PL, Macosko CW (2007) J Rheol 51:429
64. Li J, Sham LS, Kim JK, Marom G (2007) Compos Sci Technol 67:296
65. Kim S, Do I, Drzal LT (2010) Polym Compos 31:755
66. Sridhar V, Xu D, Pham TT, Mahapatra SP, Kim JK (2009) Polym Compos 30:334
67. Xu D, Sridhar V, Pham TT, Kim JK (2008) E-polymer 23:1
68. Jana S, Zhong WH (2009) Mater Sci Eng A 525:138
69. Min C, Yu D (2010) Polym Eng Sci 50:1734
70. Sridhar V, Chaudhary RNP, Tripathy DK (2006) J Appl Polym Sci 100:3161
71. Kalaitzidou K, Fukushima H, Miyagawa H, Drzal LT (2007) Polym Eng Sci 47:1796
72. Kim S, Seo J, Drzal LT (2010) Composites A 41:581
73. Jiang X, Drzal LT (2010) Polym Compos 31:1091
74. Li J, Vaisman L, Marom G, Kim JK (2007) Carbon 45:744
75. Chen D, Yang J, Chen G (2010) Compos : Part A 41:1636
76. Kim IH, Jeong YG (2010) J Polym Sci B 48:850
77. Wang L, Chen G (2010) J Appl Polym Sci 116:2029
78. Kim S, Do I, Drzal (2009) Macromol Mater Eng 294:196
79. Kai W, Hirota Y, Hua L, Inoue Y (2008) J Appl Polym Sci 107:1395
80. Knauert ST, Douglas JF, Starr FW (2007) J Polym Sci B 45:1882
81. Lee SE, Choi O, Hahn HT (2008) J Appl Phys 104:033705
82. Wang WP, Pan CY (2004) Polym Eng Sci 44:2335
83. Green M, Maron G, Li J, Kim JK (2008) Macromol Rapid Commun 29:1254
84. Srivastava NK, Mehra RM (2008) J Appl Polym Sci 109:3991
85. Weng W, Chen G, Wu D, Chen X, Lu J, Wang P (2004) J Polym Sci B 42:2844
86. Du XS, Xiao M, Meng YZ, Hay AS (2004) Polymer 45:6713
87. Du X, Xiao M, Meng YZ (2004) Eur Polym J 40:1489
88. Al-Saleh MH, Sundararaj U (2009) Carbon 47:2
89. Zheng C, Fan Z, Wei T, Luo G (2009) J Appl Polym Sci 113:1515
90. Kalaitzidou K, Fukushima H, Askeland P, Drzal LT (2008) J Mater Sci 43:2895. doi:10.1007/s10853-007-1876-3
91. Mo Z, Shi H, Chen H, Niu H, Zhao Z, Wu Y (2009) J Appl Polym Sci 112:573
92. Lin W, Xi X, Yu C (2009) Synth Met 159:619
93. Tang Q, Wu J, Li Q, Lin J (2008) Polymer 49:5329
94. Lu J, Chen X, Lu W, Chen G (2006) Eur Polym J 42:1015
95. Lu J, Weng W, Chen X, Wu D, Wu C, Chen G (2005) Adv Funct Mater 15:1358
96. Li L, Luo Y, Li Z (2007) Smart Mater Struct 16:1570
97. Fuan He, Lau S, Chan HL, Fan JT (2009) Adv Mater 21:710
98. Shen Y, Li Y, Li M, Nan CW (2007) Adv Mater 19:1418
99. Shen Y, Lin Y, Nan CW (2007) Adv Mater 17:2405
100. Yang C, Lin Y, Nan CW (2009) Carbon 47:1096
101. Sun LL, Li B, Mitchell G, Zhong WH (2010) Nanotechnology 10:305702
102. Wong SC, Wouterson EM, Sutherland EM (2006) J Vinyl Addit Technol 12:127
103. Causin V, Marega C, Marigo A, Ferrara G, Ferraro A (2006) Eur Polym J 42:3153
104. Sun X, Ramesh P, Itkis ME, Bekyarova E, Haddon RC (2010) J Phys Condens Matter 22:334216
105. Hung MT, Choi O, Ju YS, Hahn HT (2006) Appl Phys Lett 89:023117
106. Uhi FM, Yao Q, Wilkie CA (2005) Polym Adv Technol 16:533
107. Fan Z, Zheng C, Wei T, Zhang Y, Luo G (2009) Polym Eng Sci 49:2041
108. Wei T, Song L, Zheng C, Wang K, Yan J, Shao B, Fan Z (2010) Mater Lett 64:2376
109. Li J, Wong PS, Kim JK (2008) Mater Sci Eng A 483–484:660
110. Kumar S, Sun LL, Caceres S, Li B, Wood W, Perugini A, Maguire RG, Zhong WH (2010) Nanotechnology 21:105702